

Transport properties of bismuth in quantizing magnetic fields

J. H. Mangez,* J. P. Issi, and J. Heremans*

Université Catholique de Louvain, Laboratoire PCES, Place Croix du Sud 1, B-1348 Louvain-la-Neuve, Belgium

(Received 3 June 1976)

After the early work of Steele and Babiskin, low-temperature transport properties in bismuth at high magnetic fields have been used to investigate the band structure, and only the periods in the quantum oscillations were of interest. In this paper, both the amplitude of the oscillations and the magnitude of the monotonic transport components (magnetoresistance, Hall, magneto-Seebeck, and Nernst) are investigated in the liquid-helium range, where phonon drag dominates the zero-field transport properties. Measurements are extended to the quantum regime where only a few of the electron levels are occupied. Experimental results on four transport components in the low-temperature range ($T < 7$ K) and with transverse magnetic inductions up to $B = 5$ T are reported. The amplitudes of the oscillations in the magneto-Seebeck component are in good qualitative agreement with those predicted by a recent quantum transport theory.

I. INTRODUCTION

Early measurements of the thermomagnetic properties of bismuth at high magnetic fields¹ showed a strong dependence upon the magnetic field, both in the amplitude of the oscillations and in the monotonic part of the curves. These experiments were carried out on a single crystal grown from 99.99% pure bismuth, with magnetic inductions up to $B = 1.3$ T. At that time, little was known about the band structure of bismuth, and no specific reference to it was made in the analysis of the results. However, the authors noted the large increase in the thermoelectric power with magnetic field. The availability of high-purity samples, grown from 99.9999% pure bismuth, and higher magnetic fields prompted us into a detailed experimental study of the high-field ($B \leq 5$ T) thermomagnetic properties of pure bismuth in the low-temperature region ($T \leq 7$ K).

Several features make this low-temperature high-field region of interest. First, it is known² that the phonon drag in bismuth is most prominent in the liquid-helium range. In other materials like InSb,³ and graphite,⁴ the large increase in thermoelectric power with magnetic field is believed to be due to phonon-drag effects. It was worthwhile investigating if bismuth showed a similar behavior. Also, with its light effective masses, bismuth appears to be a good material for quantum limit transport measurements. The band structure of bismuth at high magnetic fields has been investigated in detail⁵ by other methods (magnetoreflexion). On the other hand, a model for the transport properties in quantizing magnetic fields, assuming isotropic parabolic bands, has been worked out.⁶ This is applicable to our experimental results, if the nonparabolicity of the electron band is taken into account.

In most theoretical models, the thermomagnetic

effects (magneto-Seebeck and Nernst) are expressed in terms of the galvanomagnetic coefficients (magnetoresistance and Hall). But it is well known that the transport properties of bismuth in the liquid-helium temperature range are very sensitive to sample purity and size,⁷ and it may be misleading to test a theory using thermo and galvanomagnetic data obtained by different groups in different conditions. Therefore, we designed our sample holder to enable us to measure both thermo and galvanomagnetic components, on the same sample, in the same experimental conditions.

In this paper, we report experimental results on four magnetotransport components, at low temperature ($T < 7$ K) and up to $B = 5$ T.

II. EXPERIMENTAL

Our sample was cut from a large single crystal grown by Brown⁸ and kindly supplied by S. Koenig and R. Brown. The sample was spark cut into a plate 4 mm thick, then cleaved at nitrogen temperature. This long rectangular bar was cut to a suitable length with a jeweller's saw. Surface damage was removed by chemical etching using nitric acid-acetic acid-water 6:6:1. The same sample was used twice. First with the magnetic field along the trigonal axis; it was then 24 mm long along the binary axis and 1.8×3.3 mm² in section with faces normal to a bisectrix and a trigonal axis. The residual resistivity ratio $\rho(300 \text{ K})/\rho(4.2 \text{ K}) \approx 200$. After the first set of measurements, the same sample was etched again, to remove all traces of solder and mounted with the magnetic field along a bisectrix axis. Due to etching, the size went down to $23 \times 1.1 \times 2.2$ mm³ along the (1, 2, 3) triad.

A sample holder was designed and built to maintain the sample horizontally, with a vertical mag-

netic field normal to the longest dimension of the sample (transverse field). Special care was given to realize a noninductive thermal matching of all the measuring wires, to avoid spurious thermal emf's in the sample. Thin copper wires were attached with GE 7031 varnish on copper pillars at the coolant bath temperature, then on other copper pillars maintained at the sample temperature. All the temperature gradients were measured using gold+0.03-at. % iron versus Chromel-P thermocouples. The thermocouple junctions were thermally anchored with GE 7031 to wedge-shaped copper pieces, which in turn were soldered on the sample by means of Wood's metal. Copper wires were inbedded in the same solder strip for the voltage measurements. All emf's were measured via a Keithley 149 milli-microvoltmeter (5×10^{-9} -V input noise) and read out on a digital voltmeter.

The temperature gradients on the sample, typically 5×10^{-2} K, were measured at zero magnetic field and the same value was used to calibrate the thermomagnetic results. This obviously introduces some error, but we felt that these errors were smaller than if we monitored the temperature gradient with the magnetic field. Indeed, the change in thermopower of the gold-iron wire with field, at low temperature and high fields, is not reproducible,⁹ and depends strongly upon the mechanical and thermal "history" of the gold-iron wire, with resulting errors ranging up to 100%. Since the power supplied to the heater is kept constant, one effectively neglects the thermal magnetoresistivity of the sample by using the zero magnetic field temperature gradient to calibrate the measurements performed with the field on. Previous results¹ indicate that the thermal magnetoresistivity is not negligible at our lowest temperatures and highest fields. However, the error introduced is smaller than the uncertainty in the thermocouple calibration.

The sample holder is designed to fit into a 50-mm-bore 5-T NbTi superconducting coil from Oxford Instruments. By means of a 50-A voltage regulated power supply,¹⁰ the magnet may be operated, either in the sweeping field mode, or in the persistent mode, the latter by closing a superconducting switch across the coil and disconnecting the power supply.

The experimental procedure was as follows: we first took a few readings, with good accuracy, at selected values of the magnetic field in the persistent field mode; we then recorded continuously the measured voltage as Y and the coil current as X on a XY recorder, in the sweeping field mode. The sweep rate was kept low (0.5 T/min) and any constant voltage induced in the wires by the sweeping field was cancelled by calibrating the recorded

traces using the permanent field measurements. Since we were interested mainly in slopes and average values, and not in the period of the oscillations, the field was not calibrated at better than 10%. The linearity and reproducibility from one run to another was much better (around 1%). It was therefore valid to consider the phase difference in the quantum oscillations when comparing the different components. The field was also monitored independently by a Hall probe (Siemens RH 117).

III. RESULTS

Four transverse magnetotransport tensor components were measured simultaneously on the same sample. Using standard notation

$$E_i = \rho_{ij}(\vec{B})J_j + \alpha_{ij}(\vec{B})\nabla_j T,$$

where E_i is the electric field, \vec{B} the magnetic induction, J_j the electric current density, $\nabla_j T$ the temperature gradient, $\underline{\rho}$ the galvanomagnetic tensor, and $\underline{\alpha}$ the thermomagnetic tensor. The indices refer to the crystallographic axes: 1—binary; 2—bisectrix; 3—trigonal. The α_{ii} -type tensor component, where the electric field is parallel to the temperature gradient we call magneto-Seebeck component, and the α_{ij} -type where the electric field and thermal gradient are crossed we call Nernst component. The experimental configuration is shown in Fig. 1.

Two sets of results, from the sample, but with two different orientations are reported here. The sample was first mounted with the magnetic field in the trigonal direction and the contacts soldered on a face normal to the bisectrix axis. Figure 2 shows the magnetoresistance $\rho_{11}(B_3)$ and the Hall component $\rho_{21}(B_3)$. The monotonic part of the magnetoresistance follows roughly a B^2 law at low fields and gradually decreases to B^1 at fields of

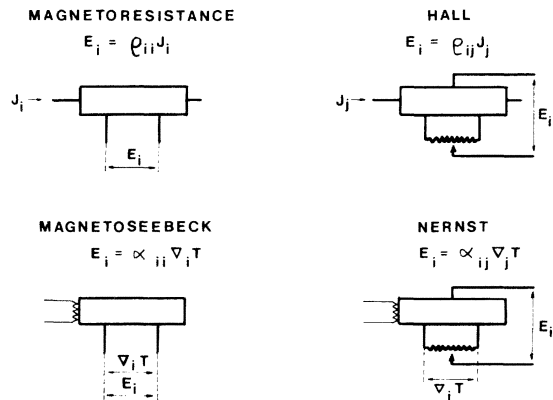


FIG. 1. Schematic experimental configuration. The magnetic field B is normal to the figure.

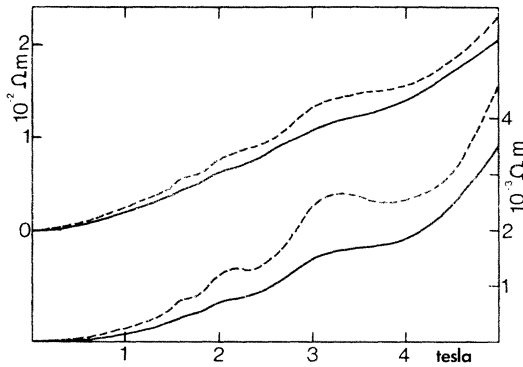


FIG. 2. Magnetoresistance $\rho_{11}(B_3)$ (upper curves, left-hand scale) and Hall component $\rho_{21}(B_3)$ (lower curves, right-hand scale). The mean temperature of the sample is $T = 4.2$ K for the dashed curves and $T = 6.8$ K for the continuous curves.

$B = 5$ T. At high fields, the magnetoresistance of bismuth in this direction is very large indeed, with $\rho_{11}(5 \text{ T}) \approx 4 \times 10^6 \rho_{11}(0)$. This large monotonic part masks the oscillatory component, but several peaks can be seen at the lowest temperature. The expected spin splitting effect in this direction¹¹ is damped at $T = 4.2$ K and can be seen only at lower temperatures ($T \approx 2.5$ K). At higher temperature ($T = 6.8$ K), the oscillations are further damped, but the monotonic component decreases slightly [(10–20)%], when the zero-field resistivity increases,¹² $\rho_{11}^0(T = 6.8 \text{ K}) \approx 2\rho_{11}^0(T = 4.2 \text{ K})$. The Hall component $\rho_{21}(B_3)$ is shown in Fig. 2. The monotonic component increases as B^2 and does not show any saturation up to $B = 5$ T. The amplitude of the quantum oscillations is larger than in the magnetoresistance because the monotonic electron and hole contributions tend to cancel each other in the Hall component, and therefore the oscillations due to the holes are clearly seen. The temperature effect, apart from the damping of the oscillations, is quite small from $T = 4.2$ K to $T = 6.8$ K.

The magneto-Seebeck component $\alpha_{11}(B_3)$ and the Nernst component $\alpha_{21}(B_3)$ are shown in Fig. 3. The effect of a field reversal on $\alpha_{11}(B_3)$ will be discussed in Sec. IV. The monotonic $\alpha_{11}(B_3)$ is large [(10^2 – 10^3) $\alpha_{11}(0)$ for $B = 5$ T], and increases linearly with the field up to $B = 4$ T. There may be a saturation at higher fields. The oscillatory component is almost washed out at the highest temperature. Unlike the galvanomagnetic components, the temperature dependence of the thermomagnetic components is large in the phonon-drag region. The magneto-Seebeck component for $B = 5$ T increases from $-1.6 \times 10^{-3} \text{ V K}^{-1}$ at 4.2 K to $-3.8 \times 10^{-3} \text{ V K}^{-1}$ at 6.8 K. Exploratory measurements indicate that $\alpha_{11}(B_3)$ decreases

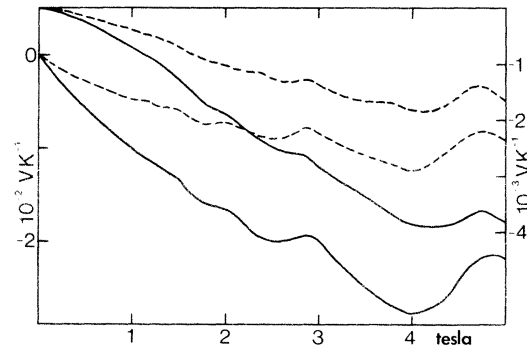


FIG. 3. Magneto-Seebeck component $\alpha_{11}(B_3)$ (upper curves, right-hand scale) and Nernst component $\alpha_{21}(B_3)$ (lower curves, left hand scale). Mean temperature $T = 4.6$ K for the dashed curves and $T = 6.8$ K for the continuous curves.

further at lower temperatures. The Nernst component $\alpha_{21}(B_3)$ is very large and equals $-2.17 \times 10^{-2} \text{ V K}^{-1}$ at 6.8 K and 5 T and is odd with magnetic field. The field dependence decreases towards saturation at the highest fields. The amplitude of the oscillations does not decrease with temperature up to $T = 6.8$ K, and the temperature dependence is similar to $\alpha_{11}(B_3)$.

The sample was then carefully cleaned and etched to remove all traces of solder, and mounted with the magnetic field along a bisectrix axis and the contacts soldered on a trigonal plane. Figure 4 shows the galvanomagnetic components $\rho_{11}(B_2)$ and $\rho_{31}(B_2)$ and Fig. 5 the thermomagnetic $\alpha_{11}(B_2)$ and $\alpha_{31}(B_2)$. The field dependences of the monotonic components are similar to those seen with the other orientation: the magnetoresistance $\rho_{11}(B_2)$ starts like B^2 and becomes linear at higher fields, the Hall $\rho_{31}(B_2)$ has a stronger B^2 dependence at all fields investigated; $\alpha_{11}(B_2)$ is linear with field and $\alpha_{31}(B_2)$ has a decreasing dependence at high fields. The oscillatory part of all four components is of course different in the two orientations. With the

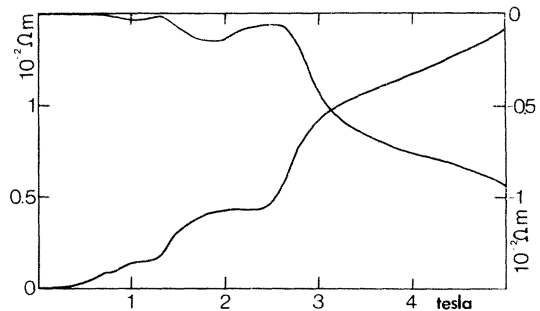


FIG. 4. Magnetoresistance $\rho_{11}(B_2)$ (lower curve, left-hand scale) and Hall $\rho_{31}(B_2)$ (upper curve, right-hand scale) at $T = 6.8$ K.

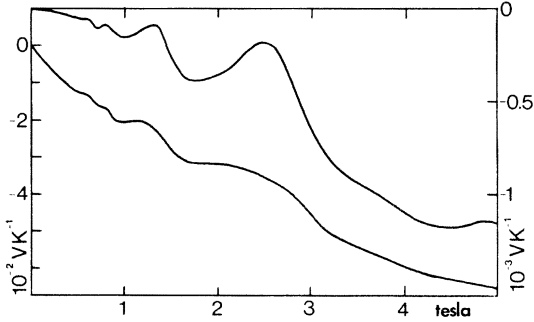


FIG. 5. Magneto-Seebeck component $\alpha_{11}(B_2)$ (upper curve, right-hand scale) and Nernst component $\alpha_{31}(B_2)$ (lower curve, left-hand scale) at a mean temperature of $T = 6.8$ K.

field in this bisectrix direction, the electron levels going through the Fermi surface result in strong oscillations up to $B \approx 2.5$ T. At higher fields, the oscillations due to large quantum number hole levels cannot be seen using our techniques.

IV. DISCUSSION

The oscillatory part of the galvanomagnetic components (Shubnikov-de Haas) has been used in the past to determine effective masses and details of the Fermi surface. Only the periods of the oscillations were used in the theoretical interpretation. The present study confirms patterns of oscillations published elsewhere.^{1,11}

This work is mainly concerned with the amplitude of the magnetotransport components in the phonon-drag region: both the amplitude of the oscillations and the field and temperature dependences of the monotonic components, at high magnetic fields, above the extreme quantum limit for some of the carriers, are of interest. Another goal of this study was to compare galvano and thermomagnetic data taken on the same sample, in the same experimental configuration. Our re-

sults for the monotonic components are summarized in Table I. The components and slopes are computed from estimated monotonic curves running through the recorded traces. The values in Table I are taken at $B = 0.5$ T because theoretical estimates based on nonquantum transport theories may be stretched up to $B = 0.5$ T. The table includes values at $B = 5$ T, the maximum magnetic field in our system. It is clear that the Nernst component is much larger than the magneto-Seebeck at all fields. Therefore, a small angle between the thermal flux and the crystal axis results in a large Nernst-type voltage which is added to the magneto-Seebeck voltage. To cancel this spurious voltage, which is odd under field reversal, we took the average of the magneto-Seebeck voltages in the two field polarities to compute the true magneto-Seebeck component, which must be even according to the crystal symmetry.¹³

A theory of the thermomagnetic effects in quantum fields has been worked out only recently.⁶ Ono's results on the oscillatory component are as follows: at temperatures where the level broadening $\gamma \ll T$, there is a large phase difference between $\underline{\rho}$ and $\underline{\alpha}$, and the amplitude of the oscillations in the magneto-Seebeck component decreases from a $B^{2.7}$ dependence to a $B^{1.4}$ dependence with increasing field. According to Ono's estimate of the level broadening $\gamma \approx 0.1$ K, we are well into the region where $\gamma \ll T$. Table II contains our estimated oscillatory components. The amplitude of the oscillations have been computed by tracing monotonic curves through the maxima and minima of the experimental results, and taking the difference. At this temperature, only a few oscillations can be seen clearly, which explains the large uncertainties in Table II. The results correlate quite well with Ono's predictions. For $\alpha_{11}(B_3)$, where the oscillations are due to hole levels crossing the Fermi surface, we find a B^2 dependence of the amplitude of the oscillations. This is smaller than the $B^{2.5}$ dependence, as predicted by Ono. For $\alpha_{11}(B_2)$, we find a $B^{1.2}$ dependence in the am-

TABLE I. Monotonic part of the measured magnetotransport components at $T = 6.8$ K.

			$B = 0.5$ T				$B = 5$ T			
			Order of magnitude	Field	Temperature	Order of magnitude	Field	Temperature		
$B \parallel 3$	$\rho_{11}(B_3)$	Magnetoresistance	$0.7 \times 10^{-3} \Omega \text{ m}$	B^2	T^0	$2 \times 10^{-2} \Omega \text{ m}$	B	T^0		
	$\rho_{21}(B_3)$	Hall	$0.4 \times 10^{-4} \Omega \text{ m}$	B^2	T^0	$3 \times 10^{-3} \Omega \text{ m}$	B^2	T^0		
	$\alpha_{11}(B_3)$	Magneto-Seebeck	$-0.2 \times 10^{-3} \text{ V K}^{-1}$	B	$T^{>1}$	$-4 \times 10^{-3} \text{ V K}^{-1}$	$B^{<1}$	$T^{>1}$		
	$\alpha_{21}(B_3)$	Nernst	$-0.6 \times 10^{-2} \text{ V K}^{-1}$	B	$T^{>1}$	$-2.5 \times 10^{-2} \text{ V K}^{-1}$	$B^{0.5}$	$T^{>1}$		
$B \parallel 2$	$\rho_{11}(B_2)$	Magnetoresistance	$0.6 \times 10^{-3} \Omega \text{ m}$	B^2	T^0	$1.4 \times 10^{-2} \Omega \text{ m}$	B	T^0		
	$\rho_{31}(B_2)$	Hall	$-0.1 \times 10^{-3} \Omega \text{ m}$	B^2	T^0	$-10^{-2} \Omega \text{ m}$	B^2	T^0		
	$\alpha_{11}(B_2)$	Magneto-Seebeck	$-0.4 \times 10^{-4} \text{ V K}^{-1}$	B	\dots	$-1.1 \times 10^{-3} \text{ V K}^{-1}$	$B^{<1}$	\dots		
	$\alpha_{31}(B_2)$	Nernst	$-1.1 \times 10^{-2} \text{ V K}^{-1}$	B	\dots	$-6.5 \times 10^{-2} \text{ V K}^{-1}$	$B^{0.5}$	\dots		

TABLE II. Oscillatory part of the measured components at $T=6.8$ K. For some components, the amplitude of the oscillations is too small to be measured accurately at this temperature.

			Amplitude of the oscillations	Phase difference
$B \parallel 3$ (holes)	$\rho_{11}(B_3)$	Magnetoresistance	...	Reference
	$\rho_{21}(B_3)$	Hall	...	No measurable lag
	$\alpha_{11}(B_3)$	Magneto-Seebeck	$B^{2 \pm 0.2}$	
	$\alpha_{21}(B_3)$	Nernst	$B^{2 \pm 0.2}$	
$B \parallel 2$ (electrons)	$\rho_{11}(B_2)$	Magnetoresistance	...	Reference
	$\rho_{31}(B_2)$	Hall	...	Phase lag
	$\alpha_{11}(B_2)$	Magneto-Seebeck	$B^{1.2 \pm 0.2}$	Phase lag
	$\alpha_{31}(B_2)$	Nernst	...	No measurable lag

plitude of the oscillations due to the last electron levels. However this cannot be interpreted in the frame of Ono's theory, since the oscillations that we detect are due to electrons in both the heavier and lighter mass directions. The phase differences are clearly seen, even at this temperature.

No predictions are made in Ono's theory for the magnitude, the field and the temperature dependence of the monotonic part of the tensor components. Ono assumes an isotropic parabolic band. Clearly, one should include the anisotropy of the band structure of bismuth, and the phonon-drag interaction in the theoretical model. Also the

strong nonparabolicity of the electron band at high magnetic fields⁵ is expected to change the field dependence of the components. More theoretical work is needed before our experimental data can be quantitatively compared with theoretical estimates.

ACKNOWLEDGMENTS

Thanks are due to Professor M. S. Dresselhaus, Dr. J. P. Michenaud, and Dr. E. Cheruvier for stimulating discussions and to P. Coopmans for preparing and mounting the samples.

*Supported by an I.R.S.I.A. grant.

¹M. C. Steele and J. Babiskin, Phys. Rev. **98**, 359 (1955).

²I. Y. Korenblit, Fiz. Tekh. Poluprovodn. **2**, 1425 (1968) [Sov. Phys.-Semicond. **2**, 1192 (1969)]; K. Sugihara J. Phys. Soc. Jpn. **27**, 356 (1969).

³S. M. Puri and T. H. Geballe, Phys. Rev. **136**, A 1167 (1964).

⁴T. Takezawa, T. Tsuzuku, A. Ono, and Y. Hishiyama, Philos. Mag. **19**, 1241 (1971).

⁵M. S. Dresselhaus, International Conference, July 24-Aug. 2, 1974, Wurzburg, Germany, p. 673-715 (unpublished).

⁶Y. Ono J. Phys. Soc. Jpn. **35**, 1280 (1973).

⁷J. P. Issi and J. H. Mangez, Phys. Rev. B **6**, 4429 (1972).

⁸R. D. Brown, IBM J. Res. Dev. **10**, 462 (1966).

⁹H. H. Sample, L. J. Neuringer, and L. G. Rubin, Rev. Sci. Instrum. **45**, 64 (1974); and private communications.

¹⁰Designed and built by H. Buyse and Y. Ducas of the Electrical Department (courants forts) of our University.

¹¹G. E. Smith, G. A. Baraff, and J. M. Rowell, Phys. Rev. **135**, A 1118 (1964).

¹²R. Hartman, Phys. Rev. **181**, 1070 (1969).

¹³Y. C. Akgoz and G. A. Saunders, J. Phys. C **8**, 2962 (1975).